PERGAMON

Mechatronics 13 (2003) 229–241

MECHATRONICS

Adaptive fuzzy logic-based velocity observer for servo motor drives

Feng-Chieh Lin, Sheng-Ming Yang *

Department of Mechanical Engineering, Tamkang University, Tamsui, Taipei Hsien 25137, Taiwan, ROC

Received 8 August 2000; accepted 19 April 2001

Abstract

As the position transducers commonly used in industry do not inherently measure an instantaneous velocity, signal processing is generally required to improve the accuracy of velocity estimation at each sampling instant. This estimated signal is then used as the velocity feedback for the velocity loop control in servo motor drives. In this paper, an adaptive fuzzy logic-based observer is proposed to estimate velocity from the measured motor position. The proposed observer has a structure similar to that of the conventional state observer except that the state feedback is replaced with a fuzzy logic feedback. The observer has two adaptation mechanisms: the first one is used to vary the fuzzy output, and the second one is used to identify the motor parameters. The experimental results show that the noise in the estimated velocity caused by the quantization of the measured position can be reduced dramatically with the proposed observer. In addition, the observer has good transient responses in both normal and in low speeds.

Keywords: Velocity observer; Adaptive fuzzy logic; Servo motor

1. Introduction

For feedback control, all high performance servo drives require both the rotor position and the velocity, and incremental encoders are the most commonly used positioning transducers in industry today. Using separate transducers for position and velocity measurement would be both mechanically difficult and also costly. Therefore it is a common practice to employ a positional transducer only, estimating the velocity from the measured position with appropriate numerical methods.

* Corresponding author. Tel.: +886-02-26215656x2769; fax: +886-02-26209745.
E-mail address: smyang@mail.tku.edu.tw (S.-M. Yang).

0957-4158/03/$ - see front matter
PII: S0957-4158(01)00044-7

The most popular numerical method is to simply take the backward difference on the measured position to approximate the differentiation of the rotor position. This method gives satisfactory results at normal and high motor speeds, but the estimated velocity becomes noisy due to the quantization of the measured position when the motor is running at low speeds [1]. In order to limit the amount of quantization noise and prevent it from causing ripples on the current command, it is necessary to filter the differentiated signal in the feedback controller. That is equivalent to reducing the bandwidth of the servo drive in order to compromise the magnitude of noise.

A number of authors have investigated the use of extra counters to extend the resolution of position measurements in order to improve velocity estimation at low speed [2–4]. Improvement of velocity estimation is achieved by measuring the elapsed time between two successive pulses coming from the encoder. Since these schemes require extra hardware and dedicated software for implementation, the cost of the system increases consequently. Several studies have been published regarding the use of closed-loop observers for velocity estimation. Lorenz and Van Patten [5] reported the use of a close-loop state observer; Bodson et al. [6] studied the use of a nonlinear close-loop observer; Brown et al. [7] proposed a least-square filtering technique; and Belanger el al. [8] proposed using Kalman filtering with constant sampling rate. These techniques are attractive since only the software modification is required to upgrade from the differentiator-based estimator, and significant reduction in quantization noise is also achieved compared to the differentiator-based estimator. However, as reported in [9], quantization noise still exists at very low speed when a state observer is used for velocity estimation.

The key design trade-off for the close-loop velocity estimators is the tracking and disturbance responses vs. the smoothness of motion at low speeds. The estimator bandwidth needs to be high to track the changes in motor position but slow to maintain smooth motion at speeds when the measured position pulse is discontinuous. In this paper, we propose a new method that uses an adaptive fuzzy logic observer for velocity estimation from position measurements.

2. State observer for velocity estimation

The equation for a differentiator-based velocity estimator can be written as

$$\tilde{\omega}(k) = \frac{\theta(kT) - \theta((k-1)T)}{T}, \tag{1}$$

where $\tilde{\omega}$ is the differentiated (measured) velocity and θ is the position, T is the sampling period, kT is the present sampling instant, and $(k-1)T$ is the previous sampling instant. Although this method is simple, however its usefulness is limited by the accuracy and quantization noise. Because in a servo motor drive, the velocity loop is the innermost state loop and its performance is generally required to be better than the outer loops, therefore its gains are also higher than the gains of the outer loops. However, the higher gain requirement for the velocity loop causes quantization noise to appear directly in the motor current command, thus limiting the

achievable bandwidth of the feedback controller and increasing power dissipation of the motor drive.

An alternative method for velocity estimation is to use a closed-loop state observer. Consider the dc motor model shown in Fig. 1, where Kt and J are the torque constant and the inertia of the motor separately, i_a is the motor current, T_d is the external disturbance, and b is the viscous friction coefficient. The model can be expressed in the following state variable form:

$$\begin{bmatrix} \dot{\theta} \\ \dot{\omega} \end{bmatrix} = \begin{bmatrix} 0 & 1 \\ 0 & -\frac{b}{J} \end{bmatrix} \begin{bmatrix} \theta \\ \omega \end{bmatrix} + \begin{bmatrix} 0 \\ \frac{Kt}{J} \end{bmatrix} i_a + \begin{bmatrix} 0 \\ -\frac{1}{J} \end{bmatrix} T_d,$$
$$\theta = [1 \quad 0] \begin{bmatrix} \theta \\ \omega \end{bmatrix}. \tag{2}$$

Rewriting Eq. (2) in a more compact form:

$$\dot{\overline{X}} = \overline{A}\overline{X} + \overline{B} i_a + \overline{D} T_d,$$
$$\overline{Y} = \overline{C}\overline{X}, \tag{3}$$

where

$$\overline{X} = \begin{bmatrix} \theta \\ \omega \end{bmatrix}, \quad \overline{A} = \begin{bmatrix} 0 & 1 \\ 0 & -\frac{b}{J} \end{bmatrix}, \quad \overline{B} = \begin{bmatrix} 0 \\ \frac{Kt}{J} \end{bmatrix}, \quad \overline{D} = \begin{bmatrix} 0 \\ -\frac{1}{J} \end{bmatrix}, \quad \text{and} \quad \overline{C} = [1 \quad 0].$$

From the model of Eq. (3), the following state velocity observer can be synthesized when the disturbance input is ignored:

$$\dot{\hat{\overline{X}}} = \overline{A}\hat{\overline{X}} + \overline{B}\,\overline{U} + \overline{K}(\overline{C}\overline{X} - \overline{C}\hat{\overline{X}}), \tag{4}$$

where $\hat{\overline{X}}(k)$ is the estimated state vector and $\overline{K} = [K1 \quad K2]$ is the gain matrix. The state velocity observer can be arranged as the block diagram shown in Fig. 2. Inputs to the observer are the measured motor position and current. The controller has a derivative and a proportional gain. The feedback controller forces error between the measured and the estimated position to zero by manipulating the input to the motor model. The damping coefficient of the observer is determined by the sum of $K1$ and b. Because b is small for typical motors, and $K1$ is generally set to a value much higher than b to increase the bandwidth of the observer, the frictional force $b\omega$ can be ignored in the synthesis of the state observer. In addition, an integral gain can also added to the observer to reduce steady-state tracking error of the estimated velocity.

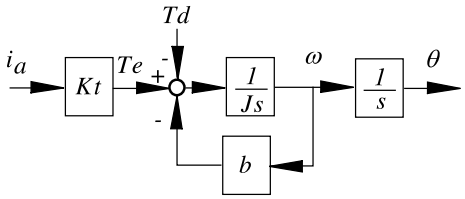

Fig. 1. Model of a dc motor.

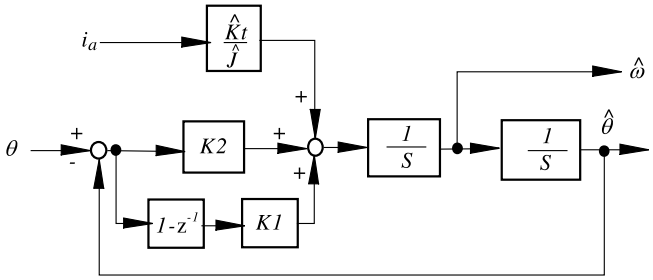

Fig. 2. Block diagram of state velocity observer.

The estimated velocity can be written as a function of the actual velocity and disturbance as follows:

$$\hat{\omega} = \frac{\left(\frac{J}{\hat{J}}\frac{\hat{K}t}{Kt}s^2 + K_1 s + K_2\right)\omega + \frac{1}{\hat{J}}\frac{\hat{K}t}{Kt}sT_d}{s^2 + K_1 s + K_2}. \tag{5}$$

It can be seen that $\hat{\omega}$ is identical to ω provided that all the motor parameters are correctly estimated. In general, the $\hat{\omega}/\omega$ response is not sensitive to motor parameters within its working frequency, i.e. bandwidth of the observer. Conversely, the $\hat{\omega}/T_d$ response is sensitive to motor parameters within the working frequency of the observer, and significant errors may occur due to external disturbances if $\hat{J}$ and $\hat{K}t$ are not correctly estimated [9].

Note that in the above analysis, the effect due to quantization of the measured motor position was not considered. In general, position quantization is not noticeable when the motor is running at normal or high speed, where the measured position per sampling period is large. However at low speeds, ripples on the estimated velocity become noticeable due to the discontinuity of the measured position pulses. These velocity ripples are undesirable since they cause an oscillatory response in the motor controller. Although it is possible to filter the velocity ripple by reducing the bandwidth of the observer at a low speed, nevertheless it complicates the implementation and tuning of the observer. In the following sections, an adaptive fuzzy observer is proposed to improve the velocity estimation.

3. Adaptive fuzzy logic-based velocity observer

Since fuzzy logic provides a nonlinear input/output mapping, hence if the regulator of the observer shown in Fig. 2 is replaced with a fuzzy logic-based regulator, then the characteristics of the observer can be designed such that it is similar to the state observer when the motor is running at normal or high speed but its bandwidth is low at low speed in order to smooth out the estimated velocity. A block diagram of the proposed fuzzy velocity observer is shown in Fig. 3. The fuzzy controller uses the position error and the rate of change of the position error as its input, and outputs a

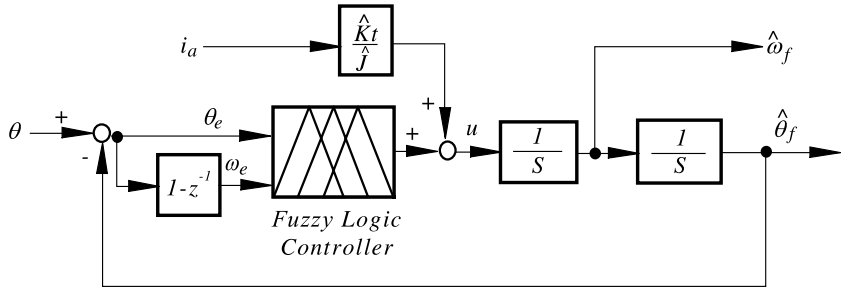

Fig. 3. Fuzzy logic-based velocity observer.

command to the motor model that forces the error between the measured and the estimated position to zero.

3.1. Fuzzy observer

The implementation of the fuzzy observer is straightforward. First, let the position and the velocity estimated by the fuzzy observer be $\hat{\theta}_f$ and $\hat{\omega}_f$, respectively, and the position and the velocity errors be $\theta_e = \theta - \hat{\theta}_f$ and $\omega_e = \tilde{\omega} - \hat{\omega}_f$. Each input to and output from the fuzzy controller has an associated set of membership functions that map the input space to a degree of membership. Each variable is partitioned into seven linguistic labels, which are: negative big (NB), negative medium (NM), negative small (NS), approximately zero (ZE), positive small (PS), positive medium (PM) and positive big (PB), respectively. When θ_e is negative (NB, NM, or NS) the estimated position is behind the actual motor position, whereas when θ_e is positive (PS, PM, or PB) the estimated position is ahead of the actual motor position. All the membership functions are triangular, and the equations for calculating the degrees of membership for a given input or output variable can be calculated from the geometry shown in Fig. 4.

The fuzzy controller has 49 rules, as shown in Table 1. The fuzzy rules are constructed according to the experience of how the control should response with respect to the position and the velocity errors in order to minimize the ripple of the estimated velocity. The center of gravity method is used for the calculation of the fuzzy controller output. Let u represents the output of the fuzzy controller. Then

$$u = \frac{\sum_{i=1}^{7} w_i c_i}{\sum_{i=1}^{7} w_i} = \frac{[\,c_1 \quad \cdots \quad c_7\,]\begin{bmatrix} w_1 \\ \vdots \\ w_7 \end{bmatrix}}{\sum_{i=1}^{7} w_i} = \overline{v}^{\mathrm{T}}\overline{w}, \tag{6}$$

where w_i is the degree of membership and c_i is the center of gravity of the ith membership function, respectively, $\overline{w}^{\mathrm{T}} = [w_1 \ \cdots \ w_7]$, and $\overline{v}^{\mathrm{T}} = [c_1 \ \cdots \ c_7]$. Although there are 49 rules, only four are used for every output value.

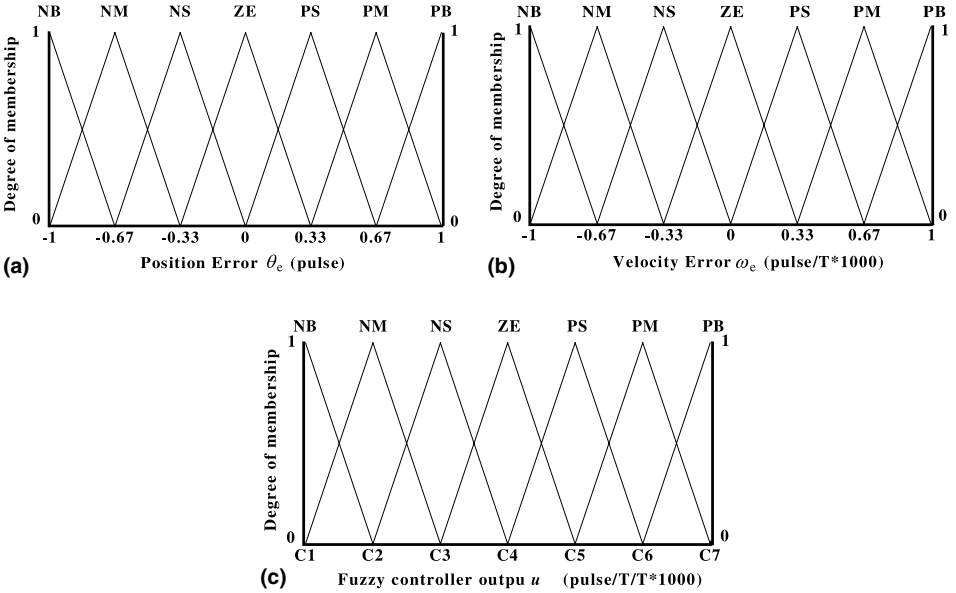

Fig. 4. Membership functions of the fuzzy velocity observer. (a) Membership function of position error input. (b) Membership function of velocity error input. (c) Membership function of output command.

Table 1
Rule base for the fuzzy velocity observer

ω_e	θ_e						
	NB	NM	NS	ZE	PS	PM	PB
PB	ZE	PS	PM	PB	PB	PB	PB
PM	NS	ZE	PS	PM	PB	PB	PB
PS	NM	NS	ZE	PS	PM	PB	PB
ZE	NB	NM	NS	ZE	PS	PM	PB
NS	NB	NB	NM	NS	ZE	PS	PM
NM	NB	NB	NB	NM	NS	ZE	PS
NB	NB	NB	NB	NB	NM	NS	ZE

3.2. Output adaptation mechanism

The fuzzy observer described above is able to smooth out the velocity estimates at low speed, however response of the observer to motor disturbance also becomes sluggish. Hence, an adaptation mechanism that automatically learns the influence of the disturbance on the observer and varies the magnitude of the fuzzy output is implemented to improve the dynamic response of the observer. Specifically, the effect of motor disturbance is tracked via θ_e and ω_e, and the range of the fuzzy output is continuously updated. Several references provide general background on adaptive fuzzy control [10,11].

Let $\hat{v}$ be the optimal range for the universe of discourse of the fuzzy output, and $\Delta\overline{v} = \overline{v} - \hat{v}$ be the parameter error vector. Equations in s-domain are used in the derivation for simplicity. From models in Figs. 1 and 3, the actual and the estimated motor velocity can be expressed as:

$$\omega = \frac{T_e}{Js} = \frac{i_a Kt}{Js}, \tag{7}$$

$$\hat{\omega}_f = \frac{i_a \hat{K}t + u}{\hat{J}s} = \frac{i_a \hat{K}t + \overline{v}^T \overline{w}}{\hat{J}s}. \tag{8}$$

If all the motor parameters are known, the rate of change of the velocity error can be obtained by combining the above equations, as

$$\dot{\omega}_e = \frac{1}{J}(-v^T \overline{w}). \tag{9}$$

Then choosing the Lyapunov function as

$$V = \frac{1}{2}(\omega_e^2 + \beta \Delta\overline{v}^T \Delta\overline{v}), \tag{10}$$

where β is a constant associated with the adaptation rate. Differentiating Eq. (10), and then substituting Eq. (9) into the resulting equation yields

$$\dot{V} = -\frac{\omega_e}{J}\hat{v}^T \overline{w} + \beta \Delta\overline{v}^T \left(\dot{\overline{v}} + \frac{\omega_e}{J\beta}\overline{w}\right). \tag{11}$$

Since $\hat{v}^T \overline{w}$ and ω_e always have the same polarity, therefore the following adaptation mechanism can be used to continuously vary the location of the output membership functions

$$\dot{\overline{v}} = -\frac{\omega_e}{J\beta}\overline{w}. \tag{12}$$

3.3. Input scaling

As the inputs to the fuzzy observer, i.e. θ_e and ω_e, vary considerably during normal motor operations, hence in order for the fuzzy observer to work properly, mapping between the input variables and their corresponding universe of discourse are scaled according to the rate of change of the position and the velocity commands. Let ω^* and α^* be the velocity and acceleration commands, respectively, and $\overline{\sigma}_\theta$ and $\overline{\sigma}_\omega$ be the input ranges for θ_e and ω_e separately under these motion commands. Then the input variables are scaled according to

$$\overline{\sigma}_\theta = m_1 \omega^* + m_2, \tag{13}$$

$$\overline{\sigma}_\omega = n_1 \alpha^* + n_2, \tag{14}$$

where m_1, n_1 are scaling factors, and m_2, n_2 are the input ranges when the motor is at rest. θ_e is scaled according to ω^* because the variation of θ_e is expected to become larger when speed increases. Similarly, ω_e is scaled according to α^* because the variation of ω_e becomes larger at higher acceleration.

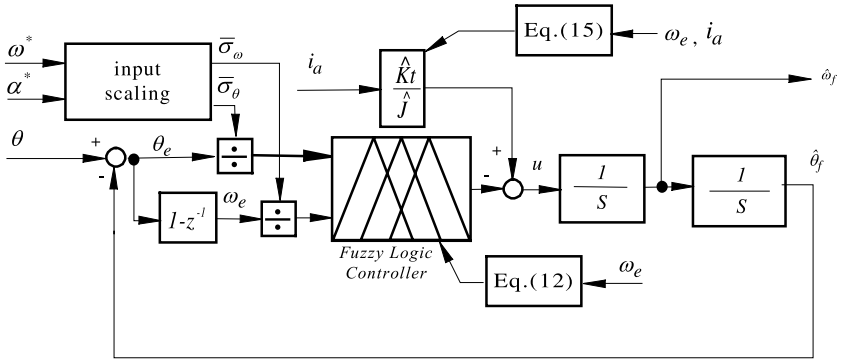

Fig. 5. Adaptive fuzzy logic-based velocity observer.

3.4. $\hat{K}t/\hat{J}$ Adaptation mechanism

As can be seen from Fig. 3, the adaptive fuzzy observer requires the knowledge of the following motor parameters: J and Kt. Though it was found in [9] that the state velocity observer is not sensitive to J and Kt within its operating frequency, however correcting $\hat{J}$ and $\hat{K}t$ can further improve the velocity estimations, particularly in the reduction of tracking errors during transient states. Also because J and Kt are grouped together in the observer, only the adaptation of $\hat{K}t/\hat{J}$ is needed. Let $\hat{k}_o$ be the nominal value of Kt/J, and $\hat{k}_c$ be the correction for $\hat{K}t/\hat{J}$. Then an adaptation rule for $\hat{k}_c$ can be derived easily from Eqs. (7) and (8) by using the MIT rule:

$$\dot{\hat{k}}_c = \beta \dot{\omega}_e i_a. \tag{15}$$

A block diagram for the fuzzy velocity observer including all the adaptation algorithms is shown in Fig. 5.

4. Experimental verifications

Several experiments were performed to evaluate the performance of the adaptive fuzzy velocity observer described in the previous sections. The motor controller was implemented with a TMS320C25 DSP controller. A 200 W dc motor was used in the experimental setup, with a 1000 lines/rev encoder mounted on the motor for position measurement. A state feedback controller was used to control the motor, with the sampling frequency set to 1000 Hz. The adaptive fuzzy observer was implemented with a PC and interfaced to the DSP digitally to furnish the velocity feedback signal. A state velocity observer was also implemented for comparison. The execution rate of the fuzzy observer was also set to 1000 Hz. A block diagram of the experimental setup is shown in Fig. 6.

Figs. 7 and 8 compare the speed responses of the control system with the measured velocity (i.e. the differentiated velocity shown in Eq. (1)), the state observer

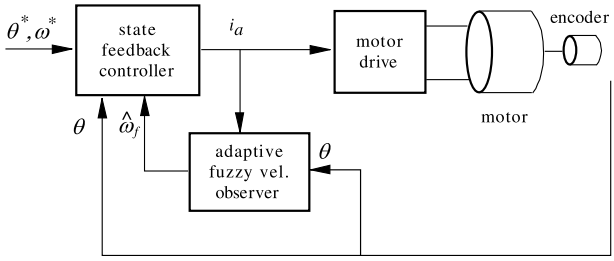

Fig. 6. Experimental system.

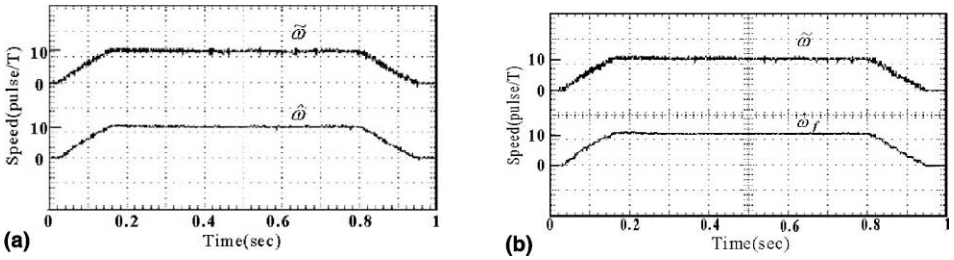

Fig. 7. Comparison of $\tilde{\omega}$ (measured velocity), $\hat{\omega}$ (estimated velocity from state observer), and $\hat{\omega}_f$ (estimated velocity from fuzzy observer) when the motor was running at 150 rpm: (a) $\tilde{\omega}$ and $\hat{\omega}$, (b) $\tilde{\omega}$ and $\hat{\omega}_f$.

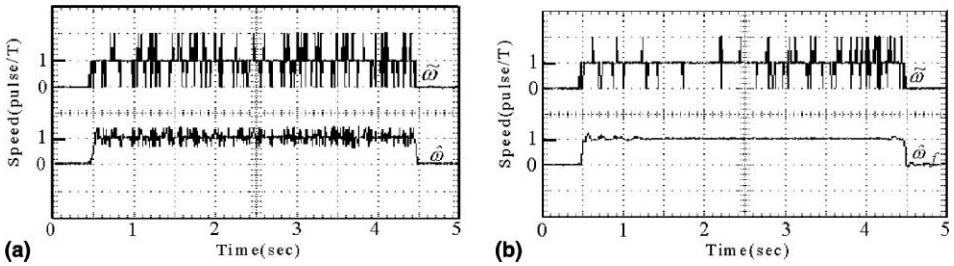

Fig. 8. Comparison of $\tilde{\omega}$, $\hat{\omega}$, and $\hat{\omega}_f$ when the motor was running at 15 rpm. (a) $\tilde{\omega}$ and $\hat{\omega}$, (b) $\tilde{\omega}$ and $\hat{\omega}_f$.

velocity, and the adaptive fuzzy observer velocity were used as the velocity feedback signal, respectively. The motor was running from 0 to 150, and 15 separately for these figures. Note that in our experimental system, 15 rpm corresponds to 1 pulse/sampling period. It can be seen that the quantization effect of the measured velocity becomes more noticeable as the motor speed gets lower. For example, in Fig. 8 $\tilde{\omega}$ only has three discrete levels due to quantization of the position measurements. On the other hand, both the state and fuzzy observers are able to track the motor velocity with relatively high accuracy when the motor is running at 150 rpm. But at 15 rpm, it is apparent that the response with the adaptive fuzzy observer velocity is superior to the response with the state observer velocity.

Similar comparisons were made when the motor was running at 3.75 rpm (0.25 pulse/T), and the results are shown in Fig. 9. Note that the measured position pulses are discontinuous when the motor speed is below 0.5 pulse/T. As shown in Fig. 9(a), $\hat{\omega}$ is oscillatory due to the discontinuous position inputs. The estimated velocity increased quickly when a position pulse was detected, and decayed exponentially when no position pulse was detected in the following sampling instants. Conversely, as shown in Fig. 9(b), the velocity estimated from the adaptive fuzzy observer, i.e. $\hat{\omega}_f$, was very smooth and almost no ripple can be found in the velocity response.

Figs. 10 and 11 compare the responses of the control system when the motor was accelerating to 0.5 pulse/T and decelerating down to 0 pulse/T using the state observer velocity and adaptive fuzzy observer velocity as its speed feedback, respectively. Again, it can be seen that the responses with the adaptive fuzzy observer are much better than with the state observer.

The effects of the output adaptation and input scaling to the fuzzy velocity observer were also examined experimentally. The center of gravity vector ($\bar{v}$) was set to 150% and 50% of its optimal value ($\hat{v}$) when the motor was running at 15 rpm. Then the responses of $\hat{\omega}_f$ were recorded and are shown in the upper two traces of Fig. 12. In addition, the input scaling factor for ω_e, i.e. $\bar{\sigma}_\omega$, was also set to 150% and 50% of its correct value when the motor was running at 15 rpm, and $\hat{\omega}_f$ was recorded and

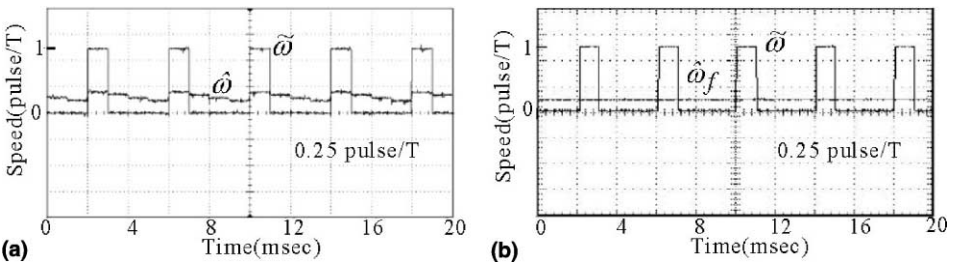

Fig. 9. Comparison of $\tilde{\omega}$, $\hat{\omega}$, and $\hat{\omega}_f$ when the motor was running at 3.75 rpm (0.25 pulse/T): (a) $\tilde{\omega}$ and $\hat{\omega}$, (b) $\tilde{\omega}$ and $\hat{\omega}_f$.

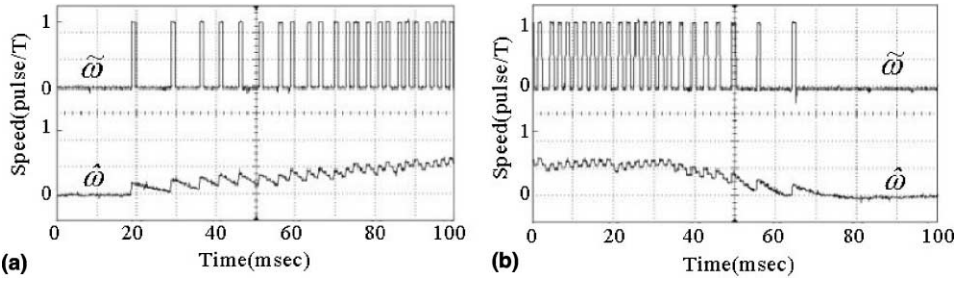

Fig. 10. Measured velocity ($\tilde{\omega}$) vs. estimated velocity from state observer ($\hat{\omega}$) when the motor was in acceleration/deceleration region. (a) Motor accelerating from 0 to 0.5 pulse/T. (b) Motor decelerating from 0.5 pulse/T to 0.

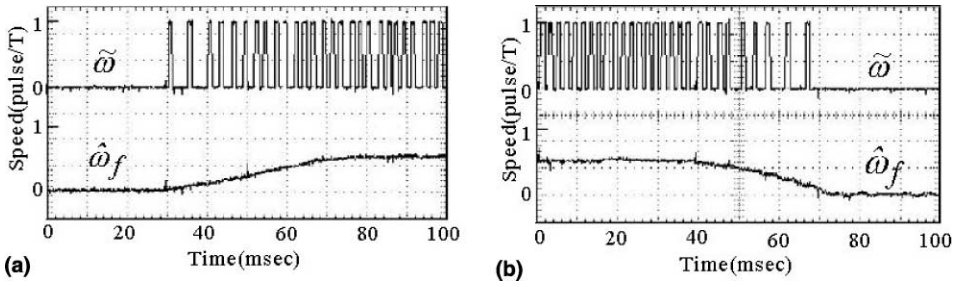

Fig. 11. Measured velocity ($\tilde{\omega}$) vs. estimated velocity from fuzzy observer ($\hat{\omega}_f$) when the motor was in acceleration/deceleration region. (a) Motor accelerating from 0 to 0.5 pulse/T. (b) Motor decelerating from 0.5 pulse/T to 0.

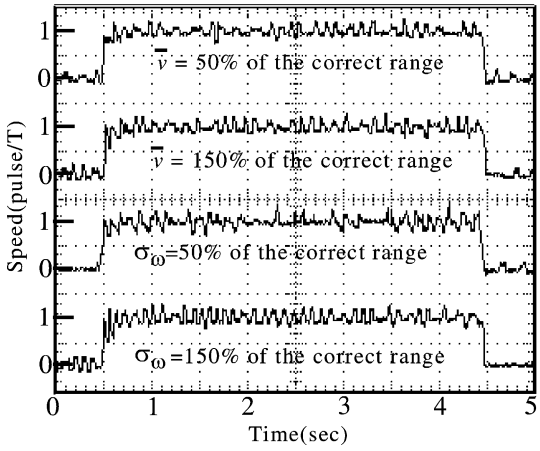

Fig. 12. Estimated velocity $\hat{\omega}_f$ when the input scaling was not properly adjusted, and the motor was running at 15 rpm.

shown in the lower traces of Fig. 12. Note that similar results will be obtained if $\overline{\sigma}_\theta$ is not set properly instead. As Fig. 12 shows, all the traces contained significant ripples. These results indicate that both the output adaptation and the input scaling do improve the fuzzy velocity estimation, however proper adjustments of these algorithms are also needed.

Finally, comparisons of the frequency spectrum of the measured velocity, the state observer velocity, and the adaptive fuzzy observer velocity are shown in Fig. 13. The motor was running at 7.5 rpm, i.e. 0.5 pulse/T, when these frequency spectra were measured. As can be seen from Fig. 13(a), the peak harmonic frequency of the measured velocity occurs around 500 Hz. This is because the sampling rate was 1000 Hz and the motor was running at 0.5 pulse/T; therefore, the processor sees a position pulse every 2 sampling periods. Similarly, the peak harmonic frequency of the state observer velocity also occurs near 500 Hz, but its magnitude is only about 1/10 of

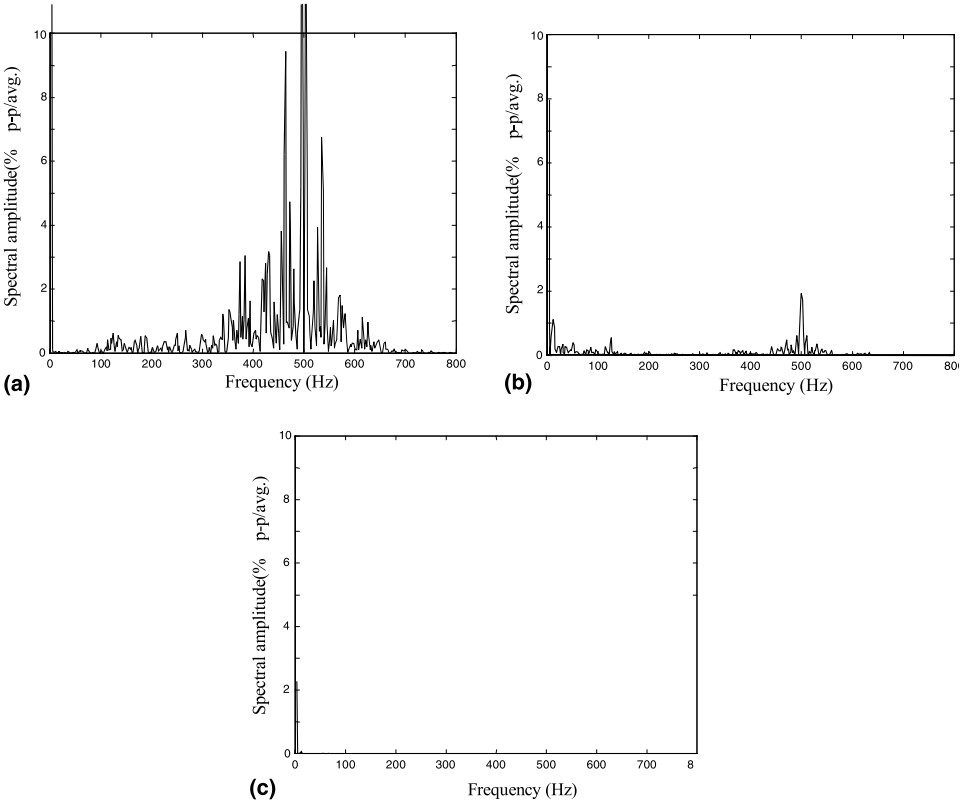

Fig. 13. Frequency spectra of the estimated velocity for various estimation techniques, with motor running at 0.5 pulse/T (7.5 rpm): (a) $\tilde{\omega}$, (b) $\hat{\omega}$, (c) $\hat{\omega}_{\mathrm{F}}$.

that of the measured velocity. On the other hand, the 500 Hz harmonic is almost unidentifiable for the adaptive fuzzy observer velocity under the same scale.

The experimental results shown in this section demonstrate the effectiveness of using the adaptive fuzzy logic-based observer to suppress velocity ripple at low speed. In addition, the results also confirmed that the adaptive fuzzy observer is superior to the state observer, particularly for low speed velocity estimation.

5. Conclusions

This paper has presented an adaptive fuzzy logic-based observer for velocity estimation from discrete position measurements for servo motor drives. The experimental results indicate that the noises in the estimated velocity caused by the quantization of measured positions can be reduced dramatically with the proposed observer. Also, because the output adaptation mechanism automatically learns the

influence of the external disturbance on the motor and the mapping between the input variables and their corresponding universe of discourse is scaled according to the rate of change of the position and the velocity commands, the velocity observer has good transient responses over the whole speed range. Thought not independently tested, the adaptation mechanism to correct $\hat{K}t/\hat{J}$ further improves the velocity estimation, particularly in the reduction of tracking errors during transient states. The results also confirm that the adaptive fuzzy observer is superior to the state observer at low speeds.

Acknowledgements

We gratefully acknowledge the support for this research by the National Science Council, Taiwan, ROC, under grant NSC 89-2213-E-032-041.

References

[1] Kavanagh RC, Murphy JM. The effects of quantization noise and sensor non-ideality on digital differentiator-bases rate measurement. IEEE Trans Instrum Meas 1998;47(6):1457–63.
[2] Sakai S, Hori Y. Ultra-low speed control of servomotor using low resolution rotary encoder. In: Proceedings of the 1995 IECON, October 1995. p. 615–20.
[3] Lemkin M, Yang, P, Huang A, Jones J, Auslander D. Velocity estimation from widely spaced encoder pulses. In: Proceedings of the 1995 American Control Conference. p. 998–1002.
[4] Galvan E, Torralba A, Franquelo LG. ASIC implementation of a digital tachometer with high precision in a wide speed range. IEEE Trans Ind Electron 1996;43(6):655–61.
[5] Lorenz R, Van Patten K. High-resolution velocity estimation for all digital, ac servo drives. IEEE Trans Ind Appl 1991;27(4):701–5.
[6] Bodson M, Chiasson J, Novotnak R. Nonlinear speed observer for high-performance induction motor control. IEEE Trans Ind Electron 1995;44(4):337–43.
[7] Brown R, Schneider S, Mulligan M. Analysis of algorithms for velocity estimation from discrete position versus time data. IEEE Trans Ind Electron 1992;39(1):11–9.
[8] Belanger PR, Dobrovolny P, Helmy A, Zhang X. Estimation of angular velocity and acceleration from shaft-encoder measurements. Int J Robotics Res 1998;17(11):1225–33.
[9] Yang SM, Ke SJ. Performance evaluation of a velocity observer for accurate velocity estimation of servo motor drives. IEEE Trans Ind Appl 2000;35(1):98–104.
[10] Cox E. Adaptive fuzzy systems. IEEE Spectrum, February 1993; p. 27–31.
[11] Wang L. Adaptive fuzzy systems and control: design and stability analysis. Englewood Cliffs, NJ: Prentice-Hall; 1994.